

Neural Data-Enabled Predictive Control

Mircea Lazar*

* *Eindhoven University of Technology, Eindhoven, Netherlands*
(e-mail: m.lazar@tue.nl)

Abstract: Data-enabled predictive control (DeePC) for linear systems utilizes data matrices of recorded trajectories to *directly* predict new system trajectories, which is very appealing for real-life applications. In this paper we leverage the universal approximation properties of neural networks (NNs) to develop neural DeePC algorithms for nonlinear systems. Firstly, we point out that the outputs of the last hidden layer of a deep NN implicitly construct a basis in a so-called neural (feature) space, while the output linear layer performs affine interpolation in the neural space. As such, we can train off-line a deep NN using large data sets of trajectories to learn the neural basis and compute on-line a suitable affine interpolation using DeePC. Secondly, methods for guaranteeing consistency of neural DeePC and for reducing computational complexity are developed. Several neural DeePC formulations are illustrated on a nonlinear pendulum example.

Keywords: Predictive control, Data-driven control, Nonlinear systems, Neural networks.

1. INTRODUCTION

Data-enabled predictive control (DeePC) (Coulson et al., 2019) is a *direct* data-driven control algorithm that utilizes data matrices to predict system trajectories and compute control actions without first identifying a parametric system model or predictor. This is very appealing for practical applications of model predictive control (MPC), as it simplifies the MPC design and implementation. For a detailed discussion on direct versus indirect data-driven methods for controller design we refer to (Markovsky et al., 2023).

A unique feature of the DeePC algorithm is that it assigns to any given predicted/future input trajectory and past inputs and outputs a *set* of predicted/future output trajectories, as explicitly pointed out in (Lazar and Verheijen, 2022, Equation (8)). This is in contrast with MPC or subspace predictive control (SPC) (Favoreel et al., 1999), which assign a unique predicted output trajectory to every predicted input trajectory. As shown in (Fiedler and Lucia, 2021), in the case of noise free data, the set of trajectories spanned by the DeePC prediction equations collapses to the same unique trajectory as MPC and SPC. However, in the case of noisy data, when SPC yields an unbiased, least squares optimal output trajectory, the set of trajectories spanned by the DeePC prediction equations is richer, and it includes the SPC one. Hence, under suitable regularization (Dörfler et al., 2023), DeePC can outperform MPC and SPC in the noisy data case, by optimizing the bias/variance trade-off.

Currently, the design, implementation and stability analysis of linear DeePC are well understood, see, for example, the recent surveys (Markovsky et al., 2023; Verheijen et al., 2023) and the references therein. However, since most real-life applications are nonlinear, there is an increasing interest in developing DeePC formulations for nonlinear systems. Several promising results in this direction include using data-driven trajectory linearization techniques (Berberich et al., 2022), kernel functions

(Huang et al., 2024) or basis functions expansion of input-output predictors (Lazar, 2023). On the other hand, many *indirect* data-driven predictive control (DPC) algorithms exist for nonlinear systems, which typically parameterize system dynamics or multi-step input-output predictors using deep neural networks (NNs), see, e.g., (Masti et al., 2020; Bonassi et al., 2021; Zarzycki and Ławryńczuk, 2022; Lazar et al., 2023). An advantage of using deep NNs is that one does not have to choose a specific kernel or basis function for representing the predictors, as the universal approximation theorem for deep NNs is valid for any Tauber-Wiener activation function (Chen and Chen, 1995). Also, there are many efficient toolboxes for training NNs (Nelles, 2020; Ljung et al., 2020) and systematic guidelines for choosing the number of hidden neurons can be found in, e.g., (Trenn, 2008). However, similarly to linear MPC or SPC, indirect neural DPC formulations assign to every future input trajectory a unique future output trajectory, corresponding to a nonlinear-least-squares-optimal neural predictor. Once trained off-line, such predictors are used on-line for prediction without exploiting newly measured data for improving predictions. Therefore, it would be of interest to develop neural-networks-based DeePC algorithms that exploit on-line measurements to optimize predictions. Alternatively, stochastic MPC methods with on-line NN model updates, see, e.g., (Pohlodek et al., 2023), could be considered.

In this paper we therefore develop a neural DeePC algorithm for nonlinear systems by merging direct and indirect approaches to data-driven control (Markovsky et al., 2023). Firstly, we point out that the outputs of the last hidden layer of a deep NN are implicitly forming a basis in a so-called *neural (feature) space* (see, e.g., (Widrow et al., 2013)), while the output linear layer performs affine interpolation in the neural space. As such, we can train *off-line* a deep NN using large data sets of trajectories to learn the neural basis and compute *on-line* a suitable affine interpolation using DeePC. We show that for linear

activation functions the original DeePC formulation is recovered, i.e., DeePC corresponds to a *linear* NN mapping.

The developed neural approach to DeePC has some desirable features compared to kernel-functions-based approaches (Huang et al., 2024), e.g., it decouples the dimension of the space in which on-line computations are performed from the number of data points. Moreover, compared to (Huang et al., 2024; Lazar, 2023) it does not require choosing a special kernel or basis function (i.e., any Tauber-Wiener activation function can be chosen (Chen and Chen, 1995)). Another contribution of this paper is the *Neural-DeePC-3* formulation defined in Problem 7, which provides a very efficient regularization method for DeePC, i.e., auxiliary variables are restricted to \mathbb{R}^{pN} (number of outputs times the prediction horizon) compared with regularization methods in (Dörfler et al., 2023; Lazar, 2023) that employ auxiliary variables in \mathbb{R}^T with $T \gg pN$ the number of data points.

2. PRELIMINARIES

Throughout this paper, for any finite number $q \in \mathbb{N}_{\geq 1}$ of vectors or functions $\{\xi_1, \dots, \xi_q\}$ we will make use of the operator $\text{col}(\xi_1, \dots, \xi_q) := [\xi_1^\top, \dots, \xi_q^\top]^\top$. As the data generating system, we consider an unknown MIMO nonlinear system with inputs $u \in \mathbb{R}^m$ and measured outputs $y \in \mathbb{R}^p$. For example, such a system could be represented using a controllable and observable discrete-time state-space model:

$$\begin{aligned} x(k+1) &= \tilde{f}(x(k), u(k)), \quad k \in \mathbb{N}, \\ y(k) &= \tilde{h}(x(k)), \end{aligned} \quad (1)$$

where $x \in \mathbb{R}^n$ is an unknown state and \tilde{f}, \tilde{h} are suitable, unknown functions. Given an initial condition $x(0)$ and a sequence of inputs $\mathbf{u}_{[0, T-1]} := \{u(0), \dots, u(T-1)\}$, the system (1) generates a corresponding output sequence $\mathbf{y}_{[1, T]} := \{y(1), \dots, y(T)\}$, which could be affected by measurement noise.

Indirect nonlinear data-driven predictive control, see, e.g., (Masti et al., 2020; Lazar et al., 2023), typically uses a multi-step predictor of the NARX type, i.e.,

$$\mathbf{y}_{[1, N]}(k) := \mathbb{F}(\mathbf{u}_{\text{ini}}(k), \mathbf{y}_{\text{ini}}(k), \mathbf{u}_{[0, N-1]}(k)), \quad (2)$$

where $\mathbb{F} := \text{col}(f_1, \dots, f_N)$ and

$$\begin{aligned} \mathbf{u}_{\text{ini}}(k) &:= \text{col}(u(k - T_{\text{ini}}), \dots, u(k - 1)) \in \mathbb{R}^{T_{\text{ini}}m}, \\ \mathbf{y}_{\text{ini}}(k) &:= \text{col}(y(k - T_{\text{ini}} + 1), \dots, y(k)) \in \mathbb{R}^{T_{\text{ini}}p}, \end{aligned}$$

and where $T_{\text{ini}} \in \mathbb{N}_{\geq 1}$ defines the order of the NARX dynamics (different orders can be used for inputs and outputs, but for simplicity we use a common order). Typically, the map \mathbb{F} is parameterized using deep neural networks. Above, $\mathbf{u}_{[0, N-1]}(k) := \{u(0|k), \dots, u(N-1|k)\}$ and $\mathbf{y}_{[1, N]}(k) := \{y(1|k), \dots, y(N|k)\}$ denote the sequence of predicted inputs and outputs at time k , respectively, based on measured data $\mathbf{u}_{\text{ini}}(k), \mathbf{y}_{\text{ini}}(k)$. Note that since each f_i is a MIMO predictor, it is the aggregation of several MISO predictors, i.e., $f_i = \text{col}(f_{i,1}, \dots, f_{i,p})$ where each $f_{i,j}$ predicts the j -th output, i.e., for $i = 1, \dots, N$

$$\begin{aligned} y_j(i|k) &= f_{i,j}(\mathbf{u}_{\text{ini}}(k), \mathbf{y}_{\text{ini}}(k), \mathbf{u}_{[0, N-1]}(k)), \\ y(i|k) &= \text{col}(y_1(i|k), \dots, y_p(i|k)), \end{aligned} \quad (3)$$

where $j = 1, \dots, p$ and p is the number of outputs.

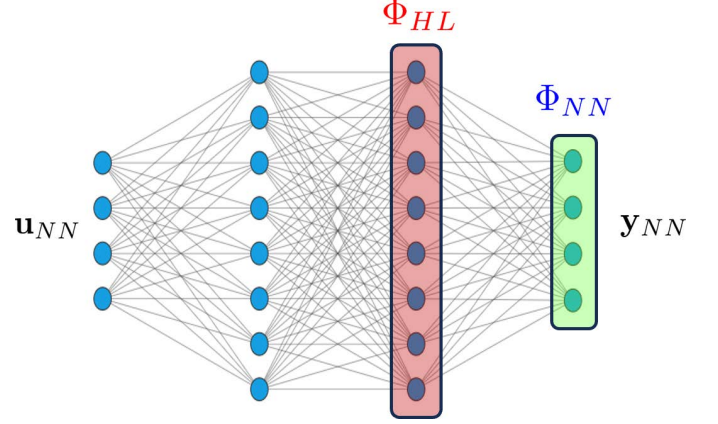


Fig. 1. Illustration of a deep MLP NN.

For any $k \geq 0$ (starting time instant in the data vector) and $j \geq 1$ (length of the data vector obtained from system (1)), define

$$\begin{aligned} \bar{\mathbf{u}}(k, j) &:= \text{col}(u(k), \dots, u(k + j - 1)), \\ \bar{\mathbf{y}}(k, j) &:= \text{col}(y(k), \dots, y(k + j - 1)). \end{aligned}$$

Then we can define the Hankel matrices:

$$\begin{aligned} \mathbf{U}_p &:= [\bar{\mathbf{u}}(0, T_{\text{ini}}) \dots \bar{\mathbf{u}}(T - 1, T_{\text{ini}})], \\ \mathbf{Y}_p &:= [\bar{\mathbf{y}}(1, T_{\text{ini}}) \dots \bar{\mathbf{y}}(T, T_{\text{ini}})], \\ \mathbf{U}_f &:= [\bar{\mathbf{u}}(T_{\text{ini}}, N) \dots \bar{\mathbf{u}}(T_{\text{ini}} + T - 1, N)], \\ \mathbf{Y}_f &:= [\bar{\mathbf{y}}(T_{\text{ini}} + 1, N) \dots \bar{\mathbf{y}}(T_{\text{ini}} + T, N)], \end{aligned} \quad (4)$$

where $T \geq (m + p)T_{\text{ini}} + mN$ is the number of columns of the Hankel matrices.

2.1 Deep neural networks

In this paper we will use deep multilayer perceptron (MLP) neural networks (Nelles, 2020) for clarity of exposition, but in principle the adopted approach is applicable to other NN types as well. To define MLP NNs we consider arbitrary Tauber-Wiener nonlinear activation functions (Chen and Chen, 1995) $\sigma : \mathbb{R} \rightarrow \mathbb{R}$ and linear activation functions, i.e., $\sigma_{\text{lin}}(s) := s$. Given an arbitrary vector $x \in \mathbb{R}^n$ we define $\bar{\sigma}(x) := \text{col}(\sigma(x_1), \dots, \sigma(x_n))$, where x_i are the elements of x . Let \mathbf{u}_{NN} and \mathbf{y}_{NN} denote the NN inputs and outputs of suitable dimensions. Next, we can define a MLP NN map $\Phi_{NN} : \mathbb{R}^q \rightarrow \mathbb{R}^p$ recursively, i.e.,

$$\begin{aligned} \mathbf{z}_1 &:= \bar{\sigma}(W_1 \mathbf{u}_{NN} + b_1), \\ \mathbf{z}_i &:= \bar{\sigma}(W_i \mathbf{z}_{i-1} + b_i), \quad i = 2, \dots, l, \\ \mathbf{y}_{NN} &:= \bar{\sigma}_{\text{lin}}(W_o \mathbf{z}_l + b_o), \end{aligned} \quad (5)$$

where $\{(W_i, b_i)\}_{i=1, \dots, l}$ are the matrices with weights and vectors with biases, respectively, of suitable dimensions, corresponding to each *hidden* layer in the deep NN and $\{(W_o, b_o)\}$ are the matrix of weights and the vector of biases of the *output* layer. The map $\Phi_{NN}(\mathbf{u}_{NN})$ can then be defined as

$$\begin{aligned} \Phi_{NN}(\mathbf{u}_{NN}) &:= \bar{\sigma}_{\text{lin}}(W_o \mathbf{z}_l + b_o) = W_o \mathbf{z}_l + b_o \\ &=: W_o \Phi_{HL}(\mathbf{u}_{NN}) + b_o, \end{aligned} \quad (6)$$

where $\Phi_{HL} : \mathbb{R}^q \rightarrow \mathbb{R}^L$ is the map defined by the composition of hidden layers. Φ_{HL} maps the deep NN inputs from a space of dimension q into a space of dimension L (dictated by the number of neurons in the last hidden layer), which we refer to as the *neural space*. Then the

total deep NN map Φ_{NN} is obtained as an affine span in the neural space. See Figure 1 for an illustration.

Remark 1. The definition (6) of Φ_{NN} as the affine span of the outputs of the hidden layer map Φ_{HL} shows that the hidden layers of a deep NN can be regarded as implicit basis functions generated by repeating two fundamental operations: affine span and passing through a scalar nonlinear activation function. In this way, by using a simple Tauber-Wiener activation function σ , a deep NN can generate a basis in the neural space, i.e., the space in which Φ_{HL} maps the NN inputs. Indeed, although not guaranteed in general, the outputs of the map Φ_{HL} are very likely to form a basis, i.e., they are linearly independent, as shown in, e.g., (Chen and Chen, 1995; Widrow et al., 2013).

3. NEURAL DEEPC

In order to build the neural DeePC controller, we need to define a neural network map $\Phi_{NN} : \mathbb{R}^{(m+p)T_{ini}+mN} \rightarrow \mathbb{R}^{pN}$ that parameterizes the multi-step input-output NARX predictor \mathbb{F} in (2) and the corresponding hidden layer map $\Phi_{HL} : \mathbb{R}^{(m+p)T_{ini}+mN} \rightarrow \mathbb{R}^L$, where $1 \leq L \leq T$ is the number of neurons in the last hidden layer. Let (\mathbf{W}, \mathbf{b}) denote all the weights and biases of all the hidden layers. Then given the Hankel data matrix

$$H := \begin{bmatrix} \mathbf{U}_p \\ \mathbf{Y}_p \\ \mathbf{U}_f \end{bmatrix} \in \mathbb{R}^{((m+p)T_{ini}+mN) \times T},$$

let $H_{:j}$ denote the j -th column of H and define the corresponding transformed matrix in the neural space as

$$\bar{\Phi}_{HL} := [\Phi_{HL}(H_{:1}) \ \Phi_{HL}(H_{:2}) \ \dots \ \Phi_{HL}(H_{:T})] \in \mathbb{R}^{L \times T}. \quad (7)$$

If (\mathbf{W}, \mathbf{b}) are fixed, then $\bar{\Phi}_{HL}$ is a data matrix and, if (\mathbf{W}, \mathbf{b}) are free variables, $\bar{\Phi}_{HL}$ is a matrix map/function. The last elements that need to be defined are the input and output vectors of the neural network, i.e.,

$$\begin{aligned} \mathbf{u}_{NN}(k) &:= \text{col}(\mathbf{u}_{ini}(k), \mathbf{y}_{ini}(k), \mathbf{u}_{[0,N-1]}(k)) \\ \mathbf{y}_{NN}(k) &:= \mathbf{y}_{[1,N]}(k). \end{aligned}$$

Next, let \mathbb{Y}, \mathbb{U} be proper polytopic sets that represent constraints, let $l_s(y, u) := \|y - y_r\|_Q^2 + \|u - u_r\|_R^2$ be a stage cost and $l_N(y)$ a terminal cost, taken for simplicity as $l_s(y, 0)$, where (y_r, u_r) are the desired output and input references and let $l_g(\mathbf{g}(k))$ be a regularization cost.

Problem 2. (Neural-DeePC-1).

$$\min_{\Xi(k)} l_N(y(N|k)) + \sum_{i=0}^{N-1} l_s(y(i|k), u(i|k)) + \lambda l_g(\mathbf{g}(k)) \quad (8a)$$

subject to constraints:

$$\begin{bmatrix} \bar{\Phi}_{HL} \\ \mathbf{1}^\top \\ \mathbf{Y}_f \end{bmatrix} \mathbf{g}(k) = \begin{bmatrix} \Phi_{HL}(\mathbf{u}_{NN}(k)) \\ 1 \\ \mathbf{y}_{[1,N]}(k) \end{bmatrix} \quad (8b)$$

$$(\mathbf{y}_{[1,N]}(k), \mathbf{u}_{[0,N-1]}(k)) \in \mathbb{Y}^N \times \mathbb{U}^N \quad (8c)$$

where $\Xi(k) := \text{col}(\mathbf{y}_{[1,N]}(k), \mathbf{u}_{[0,N-1]}(k), \mathbf{g}(k))$ are the optimization variables and $\mathbf{1}$ is a vector of ones of the same length as $\mathbf{g}(k)$, i.e., T . In principle, the hidden layers parameters (\mathbf{W}, \mathbf{b}) can also be free variables that can be computed at every time k , but then it is difficult

to guarantee that the resulting matrix $\begin{bmatrix} \bar{\Phi}_{HL} \\ \mathbf{1}^\top \end{bmatrix}$ will have

full-row rank and Problem 2 becomes very complex, and most likely not solvable in real-time on-line. Therefore, we consider that (\mathbf{W}, \mathbf{b}) are computed off-line by solving the following nonlinear least squares (NLS) problem:

$$(\mathbf{W}^*, \mathbf{b}^*, W_o^*, b_o^*) := \arg \min \left\| \mathbf{Y}_f - \bar{\Phi}_{NN}(\mathbf{W}, \mathbf{b}, W_o, b_o) \right\|_F^2 \quad (9)$$

where $\bar{\Phi}_{NN} := [\Phi_{NN}(H_{:1}) \ \Phi_{NN}(H_{:2}) \ \dots \ \Phi_{NN}(H_{:T})]$.

Consider then the following least squares problem that can be used to recompute the weights and biases of the output layer after solving the NLS (9), i.e.

$$(W_o^{LS}, b_o^{LS}) := \arg \min \left\| \mathbf{Y}_f - [W_o \ b_o] \begin{bmatrix} \bar{\Phi}_{HL}(\mathbf{W}^*, \mathbf{b}^*) \\ \mathbf{1}^\top \end{bmatrix} \right\|_F^2. \quad (10)$$

Notice that by solving the above least squares problem, i.e., after training the deep neural network using gradient descent and back propagation, we necessarily improve the data fit cost, since the new data fit cost will be either the same or lower.

Next, we define the following multi-step input-output identified predictor:

$$\mathbf{y}_{[1,N]}^{NLS}(k) := \bar{\Phi}_{NN}(\mathbf{u}_{NN}(k), \mathbf{W}^*, \mathbf{b}^*, W_o^{LS}, b_o^{LS}). \quad (11)$$

As mentioned in the introduction, differently from the above predictor, the neural DeePC predictor is in general set-valued, i.e.

$$\begin{aligned} \mathbf{y}_{[1,N]}^{N-DeePC}(k) \in \\ \left\{ \mathbf{Y}_f \mathbf{g}(k) : \begin{bmatrix} \bar{\Phi}_{HL} \\ \mathbf{1}^\top \end{bmatrix} \mathbf{g}(k) = \begin{bmatrix} \Phi_{HL}(\mathbf{u}_{NN}(k)) \\ 1 \end{bmatrix} \right\}, \end{aligned} \quad (12)$$

where the NLS optimal parameters $(\mathbf{W}^*, \mathbf{b}^*)$ are used in the map Φ_{HL} . To analyze the relation between the above defined multi-step input-output predictors we introduce the following definition.

Definition 3. Two models $\{M_1, M_2\}$ of system (1) are called equivalent if for every constraints admissible input sequence $\mathbf{u}_{[0,N-1]}$ and initial condition it holds that

$$\|\mathbf{y}_{[1,N]}^{M_1} - \mathbf{y}_{[1,N]}\| = \|\mathbf{y}_{[1,N]}^{M_2} - \mathbf{y}_{[1,N]}\|, \quad (13)$$

where $\mathbf{y}_{[1,N]}$ is the true system (1) output.

Notice that one way to establish model equivalence is to show that $\mathbf{y}_{[1,N]}^{M_1} = \mathbf{y}_{[1,N]}^{M_2}$. Next, define

$$\begin{aligned} \mathcal{S}_{\mathbf{g}} := \\ \left\{ \begin{bmatrix} \bar{\Phi}_{HL} \\ \mathbf{1}^\top \end{bmatrix}^\dagger \begin{bmatrix} \Phi_{HL}(\mathbf{u}_{NN}(k)) \\ 1 \end{bmatrix} + \hat{\mathbf{g}} : \hat{\mathbf{g}} \in \mathcal{N} \left(\begin{bmatrix} \bar{\Phi}_{HL} \\ \mathbf{1}^\top \end{bmatrix} \right) \right\}, \end{aligned}$$

where $\mathcal{N}(\cdot)$ denotes the null-space and M^\dagger denotes the pseudo-inverse of M .

Theorem 4. Consider the nonlinear least squares optimal prediction model (11) and the neural DeePC prediction model (12) defined using the same set of data $\{\mathbf{U}_p, \mathbf{Y}_p, \mathbf{U}_f, \mathbf{Y}_f\}$ generated using system (1) and the same map $\Phi_{HL}(\mathbf{W}^*, \mathbf{b}^*)$. Assume that the matrix $\begin{bmatrix} \bar{\Phi}_{HL} \\ \mathbf{1}^\top \end{bmatrix}$

has full row-rank. Let $\mathcal{E} := \mathbf{Y}_f - [W_o^{LS} \ b_o^{LS}] \begin{bmatrix} \bar{\Phi}_{HL} \\ \mathbf{1}^\top \end{bmatrix}$ be the matrix of residuals of the least squares problem (10). Then

the neural DeePC prediction model (12) is equivalent with the nonlinear least squares optimal prediction model (11) if and only if $\mathcal{E}\hat{\mathbf{g}} = \mathbf{0}$ for all $\hat{\mathbf{g}} \in \mathcal{N} \left(\begin{bmatrix} \bar{\Phi}_{HL} \\ \mathbf{1}^\top \end{bmatrix} \right)$.

Proof. From (12), it follows that

$$\begin{bmatrix} \bar{\Phi}_{HL} \\ \mathbf{1}^\top \end{bmatrix} \mathbf{g}(k) = \begin{bmatrix} \Phi_{HL}(\mathbf{u}_{NN}(k)) \\ 1 \end{bmatrix}$$

and thus all variables $\mathbf{g}(k)$ that satisfy this system of equations satisfy $\mathbf{g}(k) \in \mathcal{S}_{\mathbf{g}}$. Therefore, all predicted outputs generated by neural DeePC satisfy

$$\mathbf{y}_{[1,N]}^{\text{N-DeePC}}(k) \in \left\{ \mathbf{Y}_f \left(\begin{bmatrix} \bar{\Phi}_{HL} \\ \mathbf{1}^\top \end{bmatrix}^\dagger \begin{bmatrix} \Phi_{HL}(\mathbf{u}_{NN}(k)) \\ 1 \end{bmatrix} + \hat{\mathbf{g}} \right) : \hat{\mathbf{g}} \in \mathcal{N} \left(\begin{bmatrix} \bar{\Phi}_{HL} \\ \mathbf{1}^\top \end{bmatrix} \right) \right\}$$

Then it holds that

$$\begin{aligned} \mathbf{Y}_f \hat{\mathbf{g}} &= \left(\mathcal{E} + [W_o^{LS} \ b_o^{LS}] \begin{bmatrix} \bar{\Phi}_{HL} \\ \mathbf{1}^\top \end{bmatrix} \right) \hat{\mathbf{g}} \\ &= \mathcal{E}\hat{\mathbf{g}} + [W_o^{LS} \ b_o^{LS}] \begin{bmatrix} \bar{\Phi}_{HL} \\ \mathbf{1}^\top \end{bmatrix} \hat{\mathbf{g}} = \mathcal{E}\hat{\mathbf{g}}. \end{aligned}$$

Since $(W_o^{LS}, b_o^{LS}) = \mathbf{Y}_f \begin{bmatrix} \bar{\Phi}_{HL} \\ \mathbf{1}^\top \end{bmatrix}^\dagger$ it follows that

$$\mathbf{y}_{[1,N]}^{\text{N-DeePC}}(k) = \mathbf{Y}_f \begin{bmatrix} \bar{\Phi}_{HL} \\ \mathbf{1}^\top \end{bmatrix}^\dagger \begin{bmatrix} \Phi_{HL}(\mathbf{u}_{NN}(k)) \\ 1 \end{bmatrix} = \mathbf{y}_{[1,N]}^{\text{NLS}}(k)$$

if and only if $\mathcal{E}\hat{\mathbf{g}} = \mathbf{0}$ for all $\hat{\mathbf{g}} \in \mathcal{N} \left(\begin{bmatrix} \bar{\Phi}_{HL} \\ \mathbf{1}^\top \end{bmatrix} \right)$. \square

In general the matrix of residuals \mathcal{E} will not be identically zero, even in the case of noise free data, and thus, it is necessary to use a suitable regularization cost in neural DeePC, that penalizes the deviation of $\mathbf{y}_{[1,N]}^{\text{N-DeePC}}$ from $\mathbf{y}_{[1,N]}^{\text{NLS}}$. To this end, define the vector of variables

$$\mathbf{g}^{\text{NLS}}(k) := \begin{bmatrix} \bar{\Phi}_{HL} \\ \mathbf{1}^\top \end{bmatrix}^\dagger \begin{bmatrix} \Phi_{HL}(\mathbf{u}_{NN}(k)) \\ 1 \end{bmatrix}$$

and the regularization cost $l_g(\mathbf{g}(k)) := \|\mathbf{g}(k) - \mathbf{g}^{\text{NLS}}(k)\|_2^2$ in (8a). Indeed, in this case for $\lambda \rightarrow \infty$ in (8a) we have that $\mathbf{y}_{[1,N]}^{\text{N-DeePC}}(k) \rightarrow \mathbf{y}_{[1,N]}^{\text{NLS}}(k)$. For a finite, sufficiently large value of $\lambda > 0$ neural DeePC will optimize the bias/variance trade-off with respect to the NLS optimal predictor (11).

Remark 5. It is relatively straightforward to observe that the original DeePC algorithm for linear (or affine) systems can be recovered as a special case of neural DeePC, i.e., Problem 2. Indeed, by choosing $\sigma = \sigma_{\text{lin}}$ for all the neurons in all the hidden layers, there exists a set of weights and biases $\{(W_i, b_i)\}_{i=1, \dots, l}$ (the weights should be set equal to 0 or 1, and the biases should be set to 0) such that $\Phi_{HL}(\mathbf{u}_{NN}) = \mathbf{u}_{NN}$ and thus $\bar{\Phi}_{HL} = H$. Hence, the original DeePC algorithm corresponds to a *linear* neural network map with the hidden layer parameters fixed to specific (0 or 1) values.

3.1 Computationally efficient neural DeePC formulations

The regularization cost $l_g(\mathbf{g}(k)) := \|\mathbf{g}(k) - \mathbf{g}^{\text{NLS}}(k)\|_2^2$ is highly nonlinear and has a non-sparse structure, which leads to a computationally complex Problem 2. Therefore, consider the alternative formulation of neural DeePC.

Problem 6. (Neural-DeePC-2).

$$\min_{\Xi(k)} l_N(y(N|k)) + \sum_{i=0}^{N-1} l_s(y(i|k), u(i|k)) + \lambda l_g(\hat{\mathbf{g}}(k)) \quad (14a)$$

subject to constraints:

$$\begin{bmatrix} \bar{\Phi}_{HL} \\ \mathbf{1}^\top \end{bmatrix} \hat{\mathbf{g}}(k) = \begin{bmatrix} \mathbf{0} \\ 0 \end{bmatrix} \quad (14b)$$

$$\mathbf{Y}_f \left(\begin{bmatrix} \bar{\Phi}_{HL} \\ \mathbf{1}^\top \end{bmatrix}^\dagger \begin{bmatrix} \Phi_{HL}(\mathbf{u}_{NN}(k)) \\ 1 \end{bmatrix} + \hat{\mathbf{g}}(k) \right) = \mathbf{y}_{[1,N]}(k) \quad (14c)$$

$$(\mathbf{y}_{[1,N]}(k), \mathbf{u}_{[0,N-1]}(k)) \in \mathbb{Y}^N \times \mathbb{U}^N \quad (14d)$$

where $\Xi(k) := \text{col}(\mathbf{y}_{[1,N]}(k), \mathbf{u}_{[0,N-1]}(k), \hat{\mathbf{g}}(k))$ are the optimization variables and $l_g(\hat{\mathbf{g}}(k)) := \|\hat{\mathbf{g}}(k)\|_2^2$. It is clear that the neural DeePC formulation in Problem 6 is equivalent with the one in Problem 2, as the predicted outputs $\mathbf{y}_{[1,N]}(k)$ are equivalently parameterized in the two problems. Moreover, when $\lambda \rightarrow \infty$ in Problem 6 we obtain $\hat{\mathbf{g}}(k) \rightarrow 0$ and thus $\mathbf{y}_{[1,N]}^{\text{N-DeePC}}(k) \rightarrow \mathbf{y}_{[1,N]}^{\text{NLS}}(k)$. However, in this case, the regularization cost is greatly simplified, which improves computational efficiency.

Still, since both $\mathbf{g}(k)$ and $\hat{\mathbf{g}}(k)$ are vectors in \mathbb{R}^T , where T is the data length that can be large, especially for nonlinear systems. Therefore we propose next an alternative formulation of Problem 6, where we aim to substitute $\mathbf{Y}_f \hat{\mathbf{g}}(k)$ by a new vector of variables $\tilde{\mathbf{g}}(k) \in \mathbb{R}^{pN}$. Note that if \mathbf{Y}_f has full row-rank, we can parameterize $\hat{\mathbf{g}}(k)$ as $\mathbf{Y}_f^\dagger \tilde{\mathbf{g}}(k)$. We point out that this approach is novel also compared to the regularization methods proposed in (Lazar, 2023).

Problem 7. (Neural-DeePC-3).

$$\min_{\Xi(k)} l_N(y(N|k)) + \sum_{i=0}^{N-1} l_s(y(i|k), u(i|k)) + \lambda l_g(\tilde{\mathbf{g}}(k)) \quad (15a)$$

subject to constraints:

$$\begin{bmatrix} \bar{\Phi}_{HL} \\ \mathbf{1}^\top \end{bmatrix} \mathbf{Y}_f^\dagger \tilde{\mathbf{g}}(k) = \mathbf{0} \quad (15b)$$

$$\mathbf{Y}_f \begin{bmatrix} \bar{\Phi}_{HL} \\ \mathbf{1}^\top \end{bmatrix}^\dagger \begin{bmatrix} \Phi_{HL}(\mathbf{u}_{NN}(k)) \\ 1 \end{bmatrix} + \tilde{\mathbf{g}}(k) = \mathbf{y}_{[1,N]}(k) \quad (15c)$$

$$(\mathbf{y}_{[1,N]}(k), \mathbf{u}_{[0,N-1]}(k)) \in \mathbb{Y}^N \times \mathbb{U}^N \quad (15d)$$

where $\Xi(k) := \text{col}(\mathbf{y}_{[1,N]}(k), \mathbf{u}_{[0,N-1]}(k), \tilde{\mathbf{g}}(k))$ are the optimization variables and $l_g(\tilde{\mathbf{g}}(k)) := \|\tilde{\mathbf{g}}(k)\|_2^2$.

In Problem 7 the free variables of DeePC are now mapped into the predicted output space of dimension pN , which is typically much smaller than T . The price to pay is less free variables for optimizing the bias/variance trade-off and it is necessary that the output data matrix \mathbf{Y}_f has full row-rank. In the formulation of Problem 7, when $\lambda \rightarrow \infty$, we have that $\tilde{\mathbf{g}}(k) \rightarrow 0$ and thus $\mathbf{y}_{[1,N]}^{\text{N-DeePC}}(k) \rightarrow \mathbf{y}_{[1,N]}^{\text{NLS}}(k)$. To avoid numerical instability, slack variables can be added on the right hand side of (15b) and penalized in the cost function, as also done in linear DeePC.

4. ILLUSTRATIVE EXAMPLE

Consider the following pendulum model (Dalla Libera and Pillonetto, 2022):

$$J\ddot{\theta} = u - b\dot{\theta} - \frac{1}{2}MLg\sin(\theta), \quad (16)$$

where u and θ are the system input torque and pendulum angle, while $J = \frac{ML^2}{3}kg\ m^2$, $M = 1kg$ and $L = 1m$ are the moments of inertia, mass and length of the pendulum. Moreover, $g = 9.81m/s^2$ is the gravitational acceleration, and $b = 0.1Ns/m$ is the damping coefficient. One can model the pendulum dynamics using a state-space model discretized using Forward-Euler at $T_s = 0.033s$ as

$$\begin{aligned} \begin{bmatrix} x_1(k+1) \\ x_2(k+1) \end{bmatrix} &= \begin{bmatrix} 1 - \frac{bT_s}{J} & 0 \\ T_s & 1 \end{bmatrix} \begin{bmatrix} x_1(k) \\ x_2(k) \end{bmatrix} + \begin{bmatrix} T_s \\ J \\ 0 \end{bmatrix} u(k) \\ &\quad - \begin{bmatrix} \frac{MLgT_s}{2J} \sin(x_2(k)) \\ 0 \end{bmatrix}, \quad (17) \\ y(k) &= x_2(k), \end{aligned}$$

where $x_1(k)$ is the angular velocity $\dot{\theta}$ and $x_2(k)$ is the angle θ . We implemented and compared the performance and computational complexity of the 3 developed neural DeePC formulations, using the same data set, prediction horizon $N = 10$ and tracking cost function weights $Q = 200$ and $R = 0.5$. For all regularization costs we have used $\lambda = 1e + 4 = 10^4$. For tuning the regularization weight parameter λ we can make use of the Hanke-Raus heuristic (Hanke and Raus, 1996) and (Lazar and Verheijen, 2022, Proposition II.1), which shows that linear DeePC with Π -regularization (Dörfler et al., 2023) can be equivalently written as a regularized least squares problem. The important difference with linear DeePC is that the control input sequence $\mathbf{u}_{NN}(k)$ no longer depends linearly on $\mathbf{g}(k)$ and as such, the input related stage cost function must be omitted in the tuning procedure.

To generate the output data an open-loop identification experiment was performed using a multisine input constructed with the Matlab function `idinput`, with the parameters *Range* $[-4, 4]$, *Band* $[0, 1]$, *Period* 1000, *NumPeriod* 1 and *Sine* $[25, 40, 1]$. The data length is 1000 and $T_{ini} = 5$ is used, as estimated in (Dalla Libera and Pillonetto, 2022). An MLP NN was defined in *PyTorch* with one hidden layer with 30 neurons and with *tanh* activation function. The network was trained to find the optimal weights and biases using the *Adam* optimizer. The resulting map Φ_{HL} is used to generate a matrix $\bar{\Phi}_{HL} \in \mathbb{R}^{30 \times 990}$, since $N = 10$, the data length is 1000 and we used Hankel matrices to generate $(\mathbf{U}_p, \mathbf{Y}_p, \mathbf{U}_f)$. The resulting $\bar{\Phi}_{HL}$ matrix has full row-rank and a minimal singular value of 0.0188.

To compare the performance and computational complexity of all the derived data-driven predictive controllers we report the following performance indexes in Table 1: the integral squared error $J_{ISE} = \sum_{k=1}^{T_{sim}} \|y(k) - r(k)\|_2^2$, the integral absolute error $J_{IAE} = \sum_{k=1}^{T_{sim}} \|y(k) - r(k)\|_1$, the input cost $J_u = \sum_{k=1}^{T_{sim}} \|u(k)\|_1$ and the tracking cost $J_{track} = \sum_{k=1}^{T_{sim}} \|Q^{\frac{1}{2}}(y(k) - y_r(k))\|_2^2 + \|R^{\frac{1}{2}}(u(k) - u_r(k))\|_2^2$. The mean CPU time in seconds is also given in Ta-

Formulation	J_{ISE}	J_{IAE}	J_u	J_{track}	CPU (s)
<i>Neural-DeePC-1</i>	16.24	24.51	401	3759	91
<i>Neural-DeePC-2</i>	16.32	24.62	401	3777	24
<i>Neural-DeePC-3</i>	16.32	24.62	401	3776	0.39

Table 1. Performance & mean CPU time.

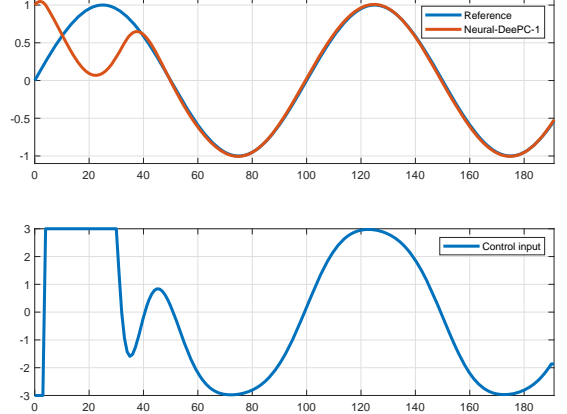


Fig. 2. Tracking performance for *Neural-DeePC-1*.

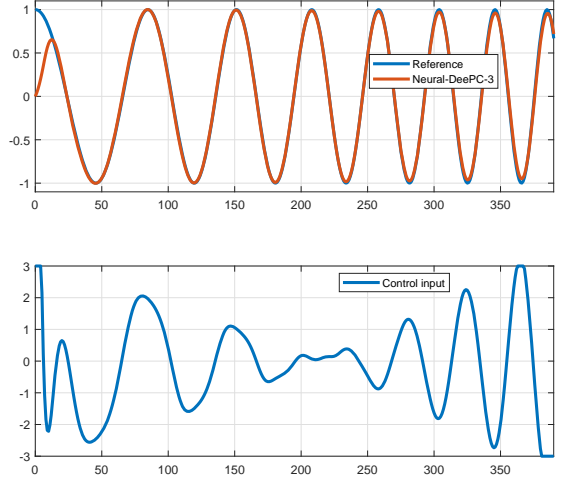


Fig. 3. Tracking performance for *Neural-DeePC-3*.

ble 1. All the predictive control optimization problem were solved with *fmincon* and a standard laptop with Intel(R) Core(TM) i7-8750H CPU 2.20GHz, 16GB RAM.

The closed-loop trajectories corresponding to *Neural-DeePC-1* are plotted in Figure 2. We observe that all the neural DeePC controllers perform well, since the obtained data is representative, the trained NN map is very accurate, and there is no noise. *Neural-DeePC-1* has slightly better performance, especially with respect to tracking performance. However, its computational complexity is much higher, which is expected, since it has 990 additional optimization variables compared to an *indirect* formulation and it uses a non-sparse regularization cost. Similar observations can be made for *Neural-DeePC-2*, which ends up being about 4 times faster than *Neural-DeePC-1*. The *Neural-DeePC-3* formulation (implemented with slack

variables in (15b) with their squared 2-norm penalized in the cost function by $1e+4$) matches the performance of the other *Neural-DPC* formulations, while achieving a much faster computation time, which is promising for real-life applications.

The performance of *Neural-DeePC-3* on a more challenging sinusoidal reference with increasing frequency is shown in Figure 3. In this case we have implemented Problem 7 without any slack variables, which led to occasional warnings, but delivered a very promising average CPU time of 0.0748 seconds.

5. CONCLUSIONS

In this paper we have constructed a formulation of data-enabled predictive control for nonlinear systems using deep neural networks. This was enabled by the key observation that the last hidden layer within a deep neural network implicitly constructs a basis for the neural network outputs. In the case of linear *DeePC*, the basis is simply formed by the system trajectories, which can be equivalently represented via a deep neural network with linear activation functions in the hidden layers. Future work will deal with data generation, training methods and architecture design for deep NNs with guarantees that the last hidden layer forms a representative basis in the space of output trajectories of dynamical systems.

ACKNOWLEDGEMENTS

The author gratefully acknowledges the assistance of MSc. Mihai-Serban Popescu with constructing and training in PyTorch the deep NNs and with generating the corresponding map Φ_{HL} for the illustrative example.

REFERENCES

- Berberich, J., Koehler, J., Muller, M.A., and Allgower, F. (2022). Linear tracking MPC for nonlinear systems Part II: The data-driven case. *IEEE Transactions on Automatic Control*.
- Bonassi, F., da Silva, C.F.O., and Scattolini, R. (2021). Nonlinear mpc for offset-free tracking of systems learned by gru neural networks. *IFAC-PapersOnLine*, 54(14), 54–59. 3rd IFAC Conference on Modelling, Identification and Control of Nonlinear Systems MICNON 2021.
- Chen, T. and Chen, H. (1995). Universal approximation to nonlinear operators by neural networks with arbitrary activation functions and its application to dynamical systems. *IEEE Transactions on Neural Networks*, 6(4), 911–917.
- Coulson, J., Lygeros, J., and Dörfler, F. (2019). Data-Enabled Predictive Control: In the Shallows of the *DeePC*. In *18th European Control Conference*, 307–312. Napoli, Italy.
- Dalla Libera, A. and Pillonetto, G. (2022). Deep prediction networks. *Neurocomputing*, 469, 321–329.
- Dörfler, F., Coulson, J., and Markovskiy, I. (2023). Bridging direct and indirect data-driven control formulations via regularizations and relaxations. *IEEE Transactions on Automatic Control*, 68(2), 883–897.
- Favoreel, W., Moor, B.D., and Gevers, M. (1999). SPC: Subspace predictive control. *IFAC Proceedings Volumes*, 32(2), 4004–4009. 14th IFAC World Congress 1999, Beijing, China, 5-9 July.
- Fiedler, F. and Lucia, S. (2021). On the relationship between data-enabled predictive control and subspace predictive control. In *IEEE Proc. of the European Control Conference (ECC)*, 222–229. Rotterdam, The Netherlands.
- Hanke, M. and Raus, T. (1996). A general heuristic for choosing the regularization parameter in ill-posed problems. *SIAM Journal of Scientific Computing*, 17(4), 956–972.
- Huang, L., Lygeros, J., and Dörfler, F. (2024). Robust and kernelized data-enabled predictive control for nonlinear systems. *IEEE Transactions on Control Systems Technology*, 32(2), 611–624.
- Lazar, M. and Verheijen, P.C.N. (2022). Offset-free data-driven predictive control. In *2022 IEEE 61st Conference on Decision and Control (CDC)*, 1099–1104.
- Lazar, M. (2023). Basis functions nonlinear data-enabled predictive control: Consistent and computationally efficient formulations. *arXiv*, 2311.05360.
- Lazar, M., Popescu, M.S., and Schoukens, M. (2023). Nonlinear data-driven predictive control using deep subspace prediction networks. In *2023 62nd IEEE Conference on Decision and Control (CDC)*, 3770–3775.
- Ljung, L., Andersson, C., Tiels, K., and Schön, T.B. (2020). Deep learning and system identification. *IFAC-PapersOnLine*, 53(2), 1175–1181. 21st IFAC World Congress.
- Markovskiy, I., Huang, L., and Dörfler, F. (2023). Data-driven control based on the behavioral approach: From theory to applications in power systems. *IEEE Control Systems Magazine*, 43(5), 28–68.
- Masti, D., Smarra, F., D’Innocenzo, A., and Bemporad, A. (2020). Learning affine predictors for mpc of nonlinear systems via artificial neural networks. *IFAC-PapersOnLine*, 53(2), 5233–5238.
- Nelles, O. (ed.) (2020). *Nonlinear System Identification From Classical Approaches to Neural Networks, Fuzzy Models, and Gaussian Processes*. Lecture Notes in Control and Information Sciences. Springer, Cham, Switzerland. Second Edition.
- Pohlodek, J., Alsmeyer, H., Morabito, B., Schlauch, C., Savchenko, A., and Findeisen, R. (2023). Stochastic model predictive control utilizing bayesian neural networks. In *2023 American Control Conference (ACC)*, 603–608.
- Trenn, S. (2008). Multilayer perceptrons: Approximation order and necessary number of hidden units. *IEEE Transactions on Neural Networks*, 19(5), 836–844.
- Verheijen, P., Breschi, V., and Lazar, M. (2023). Handbook of linear data-driven predictive control: Theory, implementation and design. *Annual Reviews in Control*, 56, 100914.
- Widrow, B., Greenblatt, A., Kim, Y., and Park, D. (2013). The no-prop algorithm: A new learning algorithm for multilayer neural networks. *Neural Networks*, 37, 182–188.
- Zarzycki, K. and Ławryńczuk, M. (2022). Advanced predictive control for gru and lstm networks. *Information Sciences*, 616, 229–254.